The ERS-2 SAR Performance: the 2004 update

P.J. Meadows [(1)] & B. Rosich [(2)]

[(1)] *BAE SYSTEMS Advanced Technology Centre, West Hanningfield Road, Great Baddow, Chelmsford, Essex, CM2 8HN, United Kingdom.*
Email: peter.meadows@baesystems.com

[(2)] *European Space Agency, Directorate of Application Programmes, ESRIN, 00044 Frascati, Italy.*
Email: betlem.rosich@esa.int

ABSTRACT

The performance of the ERS-2 Synthetic Aperture Radar (SAR) is routinely assessed at the ESA Product and Archiving Facilities (PAFs) via a variety of quality assessment and calibration measures. This paper gives the latest ERS-2 SAR quality assessment and calibration results including updates to ERS-2 SAR internal calibration and stability, noise equivalent radar cross-section measurements, updates to the ERS-2 nominal replica pulse correction table and image localisation results. Equations are given for the calculation of distributed and point targets from PRI and SLC products. Also given are ERS-2 attitude and SAR Doppler variations following the change from three to one gyroscope operations in February 2000 and the change to gyro-less operations in February 2001.

INTRODUCTION

The ERS-2 SAR mission has been in operation since April 1995. It, along with ERS-1 [1], has fully lived up to its expectations by successfully demonstrating the ability of imaging radars to provide valuable long-term earth observation data to many categories of users.

Users require the SAR products from the ERS-2 SAR to be calibrated (absolutely or relatively). Absolute calibration supports the geophysical interpretation of SAR data by relating the digital values in data products to the physical and meaningful estimation of the normalised radar cross-section σ^o (also referred to as the backscattering coefficient). Relative calibration enables SAR products from either ERS-1 or ERS-2 to be compared with each other. The importance of using calibrated ERS SAR imagery has been demonstrated for the application of ocean wind speed extraction [2] and land applications [3, 4].

ELEVATION ANTENNA PATTERN

The in-orbit ERS-2 SAR elevation antenna pattern was estimated using the Amazon rainforest. This was derived by using the mean range profile of several images of uniform rainforest and assuming that γ (= $\sigma^0/\cos(\alpha)$ where σ^0 is radar cross-section and α is incidence angle) is constant across the SAR swath. The derived elevation antenna pattern is shown in Fig. 1. Improvements to the implementation of the elevation pattern in the ESA VMP processors at extreme near and far ranges were made in November 2001 (VMP v6.8). Tables giving both patterns can be found in [5].

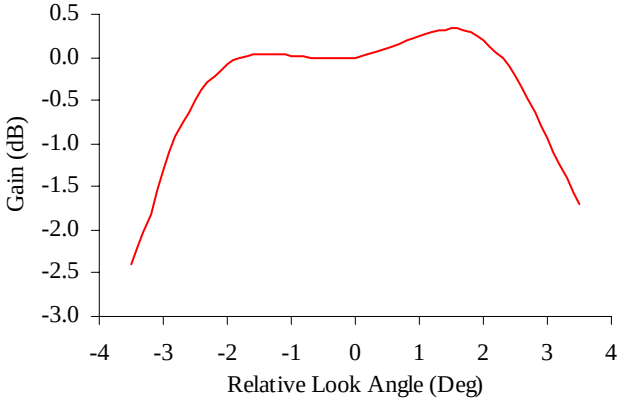

Fig. 1. ERS-2 SAR elevation antenna pattern (2-way gain)

QUALITY ASSESSMENT

The quality of ERS-2 SAR imagery has been assessed via impulse response function (IRF) measurements using the three ESA transponders deployed in The Netherlands. These measurements include the azimuth and range spatial resolutions, peak sidelobe ratio and integrated sidelobe ratio (see [2] for definitions). Table I gives values for these parameters from the PRI and SLCI products; as the PRI product range resolution varies across the swath, the table gives the range resolution converted to an incidence angle of 23° (i.e. as if all the transponders were at an incidence angle of 23°). The PRI results have been derived from measurements up to December 2001 (when the remaining ESA transponder stopped operating) while the SLCI results are derived from a set of 10 products acquired between August 1995 and February 1997. Fig. 2(a) shows the PRI azimuth resolution as a function of acquisition date and Fig. 2(b) shows the range resolution as a function of incidence angle for ERS-2 PRI products. The solid line and curve in these figures show the theoretical spatial resolutions. In addition, Fig. 2(c) and 2(d) show the peak and integrated sidelobe ratios as a function of acquisition date for ERS-2 PRI products. Note that the largest azimuth and range resolution value is from a de-focussed image acquired during the Extra Backup Mode in February 2001 (see section on attitude and Doppler variations below). Table I excludes the spatial resolutions from this scene.

Table I and Fig. 2 show that the measured azimuth and range resolutions compare well with theoretical values (20.76m for PRI azimuth resolution, 24.67m for PRI range resolution at 23° incidence angle, 4.82m for SLCI azimuth resolution and 9.64m for SLCI slant range resolution). The sidelobe ratios are all low and acceptable.

Parameter	PRI	SLCI
Azimuth resolution	21.63±0.37m	5.33±0.03m
Range resolution	25.19±0.41m	9.83±0.07m
Peak sidelobe ratio	-15.8±0.7dB	-21.9±0.6dB
Integrated sidelobe ratio	-12.2±1.4dB	-14.9±0.5dB

Table I. ERS-2 SAR PRI and SLCI image quality parameters derived from the ESA transponders

The ESA transponders have also been used to derive the point target azimuth ambiguity ratio when the ambiguity background is sufficiently low to enable a measurement to be made (see [2] for further details). Based on the measurement of 10 ERS-2 SAR ambiguities in PRI products, the average azimuth ambiguity ratio is -24.5±2.9dB while the average difference in the measured and theoretical azimuth locations of the ambiguities is only 4.1±2.2m (i.e. less than one pixel). These results indicate an excellent ambiguity performance for the ERS-2 SAR.

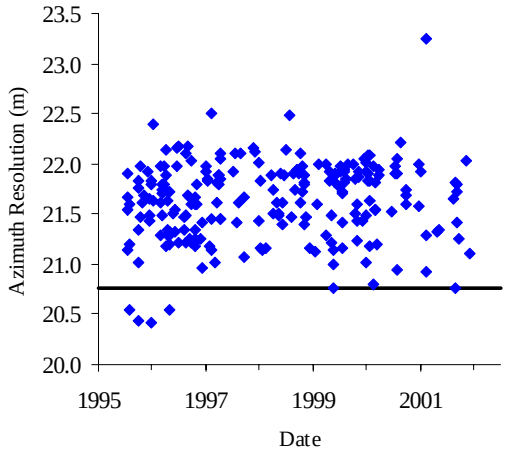

Fig. 2(a). ERS-2.SAR.PRI azimuth resolution derived from the ESA transponders (the line is the theoretical azimuth resolution)

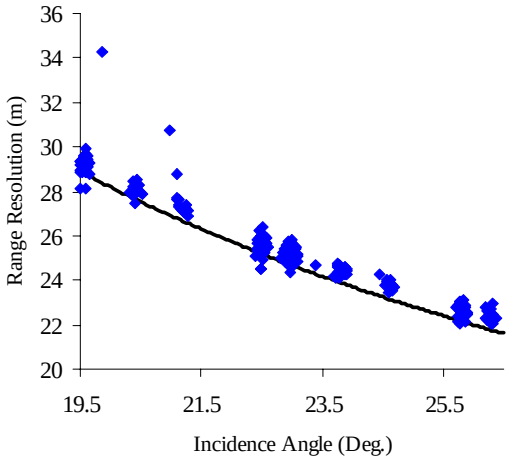

Fig. 2(b). ERS-2.SAR.PRI range resolution derived from the ESA transponders (the curve is the theoretical range resolution)

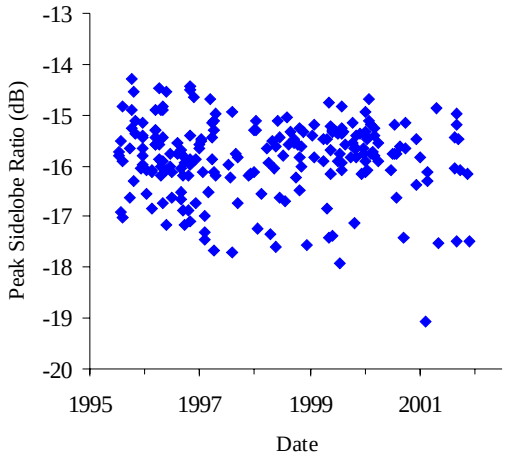

Fig. 2(c). ERS-2.SAR.PRI peak sidelobe ratio derived from the ESA transponders

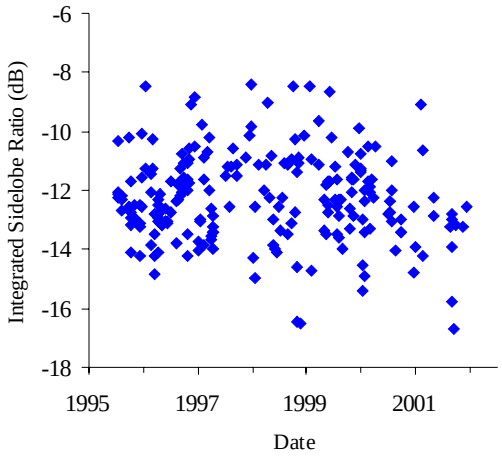

Fig. 2(d). ERS-2.SAR.PRI integrated sidelobe ratio derived from the ESA transponders

One source of additional point targets for quality assessment is ERS SAR ground receiving stations [6]. As these are used to acquire ERS SAR raw data in real time, they will be pointing towards the satellite while acquiring the data. Image quality parameters have been derived for two ground stations: the ESA ground station at Kiruna, Sweden and the German national station at Neustrelitz, Germany. The Kiruna ground station has an extremely saturated IRF with an estimated radar cross-section of ~71dBm^2 (cf. ~57dBm^2 for the ESA transponders). However, the ground station azimuth ambiguities are sufficiently strong to enable some IRF parameters to be measured. These have a radar cross-section of ~47.5dBm^2 but very little sidelobe structure is visible. The Neustrelitz ground station is not saturated in PRI products and so can be used to derive all IRF parameters. Table II gives the spatial resolution and sidelobe ratios for the two ground stations; acceptable mean values are found for the Kiruna azimuth and range resolutions and all the Neustrelitz IRF parameters (the Kiruna sidelobe ratios are poor due to lack of sidelobes in the ambiguities). The main difference between the ground station quality parameters and those derived from the ESA transponders is that the standard deviation of the measurements is greater.

Parameter	Kiruna	Neustrelitz
Azimuth resolution	22.66±0.50m	22.42±0.92m
Range resolution (at 23°)	26.74±0.69m	26.76±1.76m
Peak sidelobe ratio	-8.7±1.3dB	-15.9±1.2dB
Integrated sidelobe ratio	-4.0±1.6dB	-13.5±1.1dB

Table II. ERS-2 SAR PRI image quality parameters derived from the Kiruna and Neustrelitz ground stations

Large uniform distributed targets can be used to estimate the image radiometric resolution. ERS-2 PRI and SLCI products give radiometric resolutions of 2.07dB and 3.03dB respectively. The theoretical values are 1.98dB for the PRI product and 3.01dB for the SLCI product (these values assume perfectly uniform distributed targets).

RADIOMETRIC CALIBRATION

The radiometric calibration of ERS-2 SAR products is achieved via internal and external calibration to determine equations that can be used to calculate the radar cross-section of point and distributed targets. External calibration comprised elevation antenna pattern derivation using the Amazon rain forest and the use of the ESA transponders for derivation of the image product calibration constants. The radiometric calibration corrections for ERS-2 ADC power loss are required to be carried out by the user [2, 3, 4, 5].

Internal Calibration

The internal calibration of the ERS-2 SAR is assessed via calibration pulse, replica pulse and noise signal powers. The

calibration pulse and noise signal are available at the start and end of each imaging sequence while the replica pulses are available throughout an imaging sequence. The calibration pulse measures the majority of any gain drift from image sequence to image sequence while the replica pulse monitors any gain drift during the imaging sequence when the more representative calibration pulse is not available. In fact, the power of the calibration pulse is the best guide we have for the transmitted pulse power. The SAR processors at the PAFs make no direct use of the calibration pulse and noise signal powers while the replica pulse is used for the range compression part of the processing.

Calibration pulse, replica pulse and noise signal powers from ERS-2 SAR data archived at the UK-PAF are shown in Fig. 3. The calibration pulse powers from the start and end of imaging sequences are shown in Fig. 3(a) as a function of acquisition date. Unfortunately, the replica pulse power at the end of each imaging sequence is not calculated correctly and thus Fig. 3(b) only shows the replica powers from the start of each imaging sequence. Fig 3(c) shows the relationship between the calibration and replica pulses (from the start of imaging sequences). Finally, Fig 3(d) shows the noise power from the start of each imaging sequence (the noise power at the end of imaging sequences is not calculated correctly).

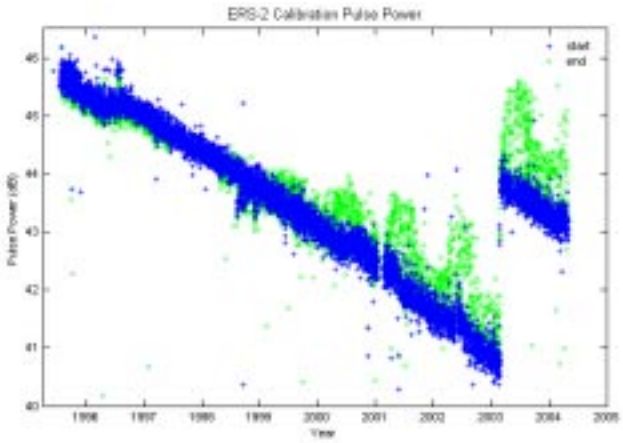

Fig. 3(a). ERS-2 SAR calibration pulse powers

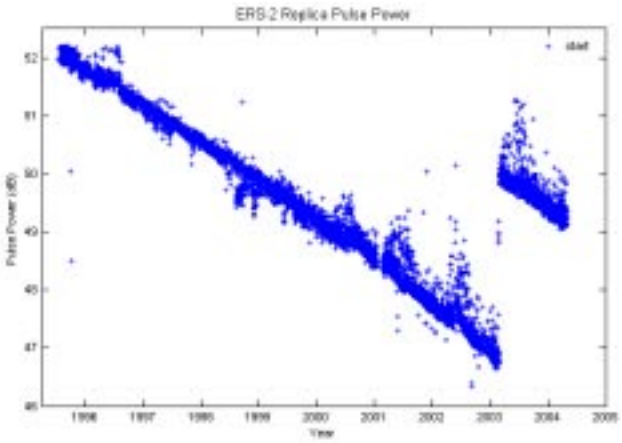

Fig. 3(b). ERS-2 SAR replica pulse powers

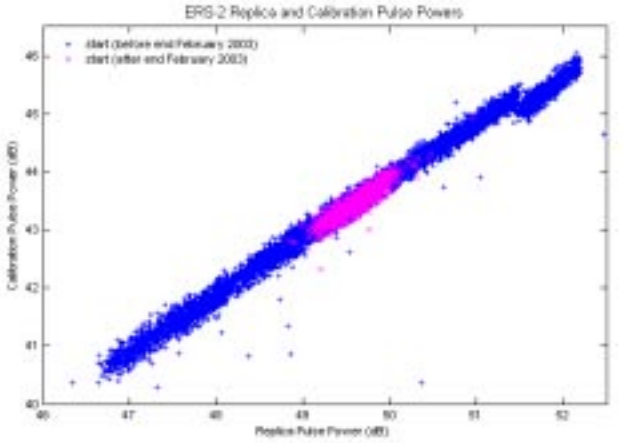

Fig. 3(c). Relationship between ERS-2 replica and calibration pulse powers. The red symbols show the replica and calibration pulse powers since the end of February 2003.

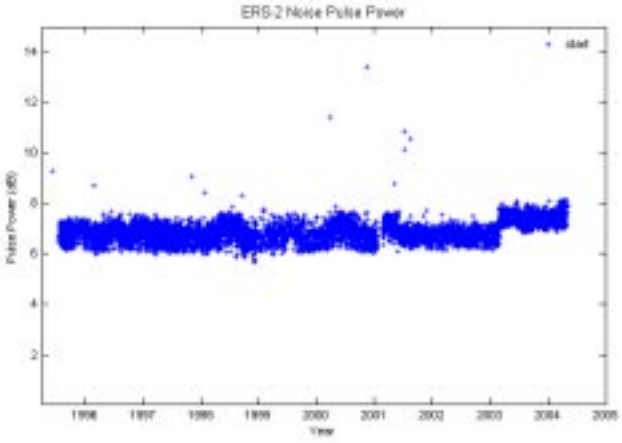

Fig. 3(d). ERS-2 SAR noise signal powers

The power of the calibration and replica pulses were increased by 2dB on 26th February 2003 and a further 1dB on 28th February 2003 through an increase in the up-convertor level and a decrease in receiver gain respectively. Prior to and following this change both the calibration and replica pulse powers show a drop in power as a function of time. The rate of decrease for both powers was approximately 0.66dB per year between launch and the end of 2000 and then approximately 0.82dB per year to the end February 2003. Since the gain change, the rate of decrease has returned to approximately 0.66dB per year. Unlike the ERS-1 SAR [1], the ERS-2 calibration and replica pulse powers are correlated (see Fig. 3(c)) and hence no replica pulse correction is required when obtaining the radar cross-section from ERS-2 SAR

imagery. This is because any reduction in transmitter power is removed by the reduced power of the replica pulse used for range compression. Note that the noise signal power remained constant up to the end of February 2003 since when it has increased slightly.

Raw Data Quality

SAR raw data obeys a certain statistical distribution: zero mean, Gaussian amplitude and uniform phase. A selection of raw data parameters are derived for all the ERS-2 SAR data archived at the UK-PAF. Fig. 4 shows the arithmetic mean, standard deviation for the in-phase (I) and quadrature (Q) channels together with saturation (the percentage of raw data samples occupying the highest or lowest quantisation levels).

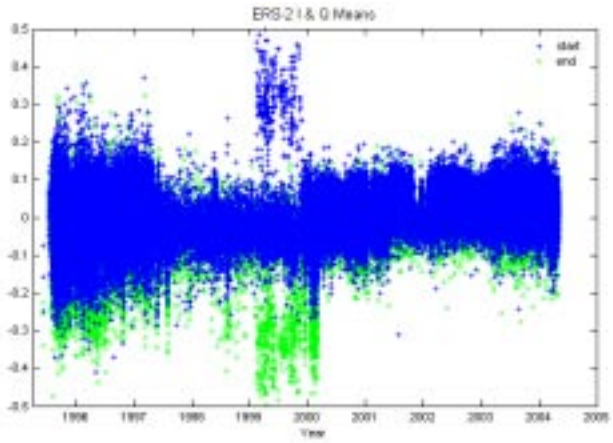

Fig. 4(a). ERS-2 SAR raw data mean

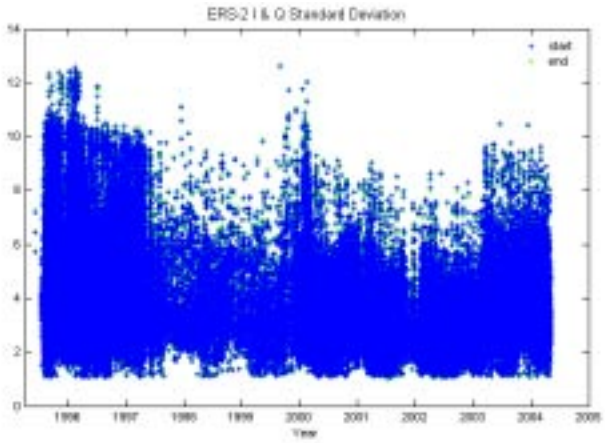

Fig. 4(b). ERS-2 SAR raw data standard deviation

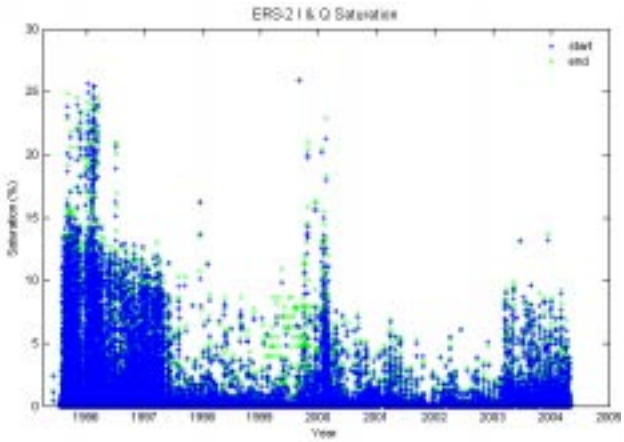

Fig. 4(c). ERS-2 SAR saturation

The I and Q mean values have been stable with very little difference between the I and Q values. As the expected mean value is zero and any difference, the bias, is removed prior to SAR processing. The standard deviation and saturation shows larger values at the start of the mission due to the reducing power of the SAR up to the gain change at the end of February 2003 when the standard deviation and saturation increased slightly. Differences between the I and Q channels, the gain imbalance, are removed prior to processing.

4.3 Stability

The stability of the ERS-2 SAR has been measured using the three ESA transponders deployed in The Netherlands. In particular, the measured radar cross-sections of the transponders have been compared to their actual radar cross-section values. This relative transponder radar cross-section (after the power loss calibration correction has been applied) has been routinely calculated as is shown in Fig. 5.

The measured mean radiometric results for the ERS-2 SAR using the ESA transponders are shown in Tables III and IV. This table indicates an excellent stability. In addition, the radiometric accuracy value is very good while the peak to peak radar cross-section value is acceptable.

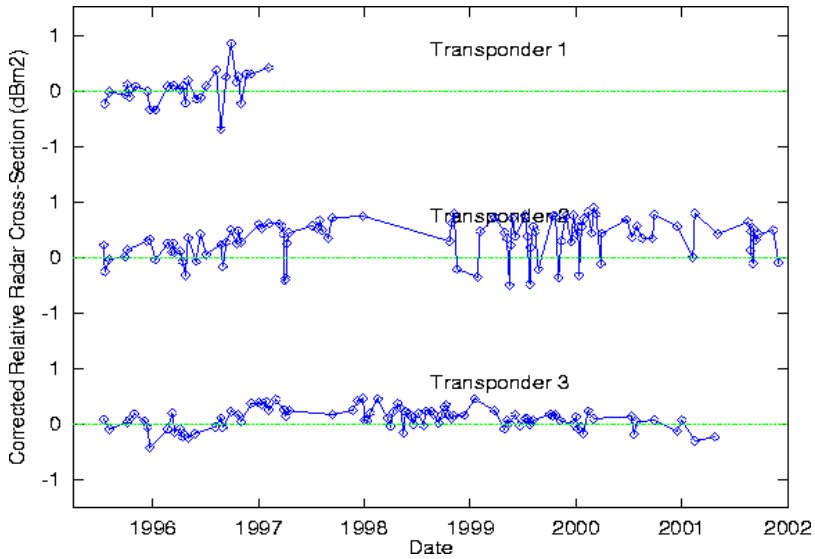

Fig. 5. ERS-2 SAR corrected relative radar cross-sections for the ESA transponders (up to December 2001).

Transponder	Acquisition Dates	Mean Accuracy (dB)	Mean Stability (dB)	Peak-Peak RCS (dB)	No of Measurements
Tran. #1	19-Jul-95 to 05-Feb-97	0.04	0.29	1.54	28
Tran. #2	19-Jul-95 to 30-Nov-01	0.33	0.34	1.39	100
Tran. #3	19-Jul-95 to 25-Apr-01	0.11	0.18	0.88	92

Table III. ERS-2 SAR radiometric results derived from the ESA transponders

Parameter	
Radiometric stability	0.27dB
Radiometric accuracy	0.16dB
Peak to peak radar cross-section	1.27dB

Table IV. Mean ERS-2 SAR radiometric results derived from the ESA transponders

The measured radar cross-section of the Kiruna ground station azimuth ambiguities have also been used to derive the stability of the ERS-2 SAR by using the average of two ambiguities in each scene. The use of the azimuth ambiguities assumes that the ERS SAR azimuth antenna pattern is stable. Table V gives the mean radar cross-section, stability and peak to peak radar cross-section values of the Kiruna ambiguities. These results are slightly higher than the transponder results given in Table IV. Fig. 6(a) and 6(b) show the ERS-2 Kiruna ambiguity radar cross-section relative to the mean value as a function of date and incidence angle. Fig. 6(b) also shows that there is no obvious radar cross-section trend with incidence angle. Note that the mean ambiguity radar cross-section derived using ERS-1 and ERS-2 imagery was found to be similar indicating a good relative radiometric calibration between the two instruments [6].

Ground Station	Acquisition Dates	Radar Cross-Section (dBm^2)	Mean Stability (dB)	Peak-Peak RCS (dB)	No of Measurements
Kiruna	20-Jul-95 to 20-Mar-04	47.87	0.57	3.05	72
Neustrelitz	13-Apr-96 to 11-Mar-04	59.01	0.51	2.97	153

Table V. ERS-2 SAR radiometric results derived from the Kiruna and Neustrelitz ground stations

Table V also gives the mean radar cross-section, stability and peak to peak radar cross-section values for the Neustrelitz ground station. Fig. 6(c) shows the ERS-2 Neustrelitz ground station radar cross-section relative to its mean value as a function of date and incidence angle. The radiometric stability and peak to peak RCS results are slightly higher than for

the ESA transponder. Examination of Fig. 6(d) shows there are five radar cross-section measurements that are significantly lower than the majority. Four of these occur when the ground station IRF is at extreme low and high incidence angles - it is suggested that the ground station itself is contributing to the larger than expected radar cross-section variations. Overall, the radiometric stability results using the Kiruna and Neustrelitz give results that are, at worst, only 5% higher than derived using the ESA transponders thus indicating that ground stations could be used as secondary calibration sources.

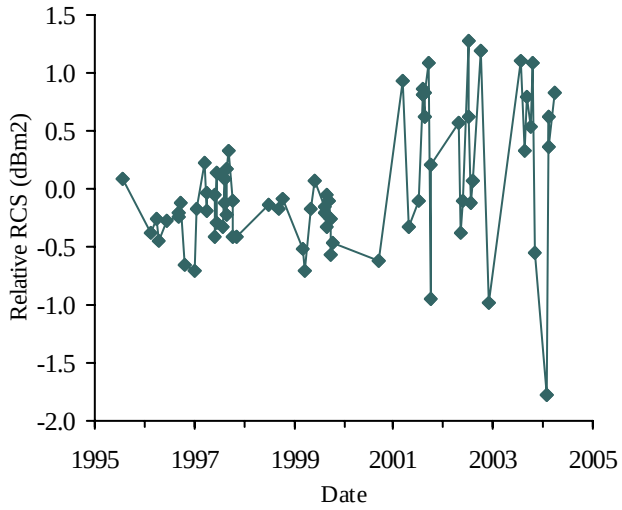

Fig. 6(a). Kiruna azimuth ambiguity relative radar cross-section as a function of date

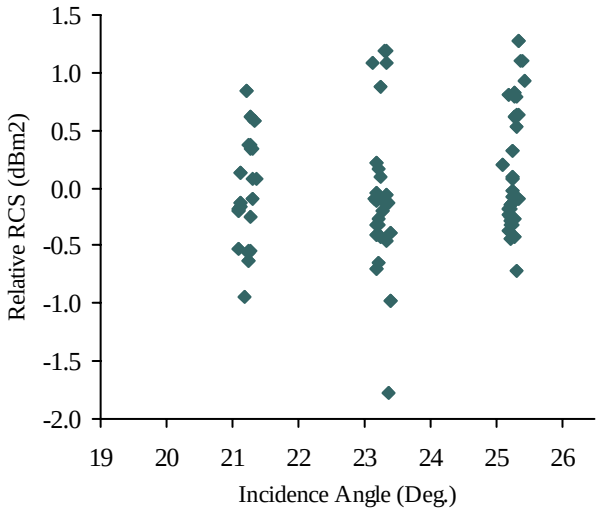

Fig. 6(b). Kiruna azimuth ambiguity relative radar cross-section as a function of incidence angle

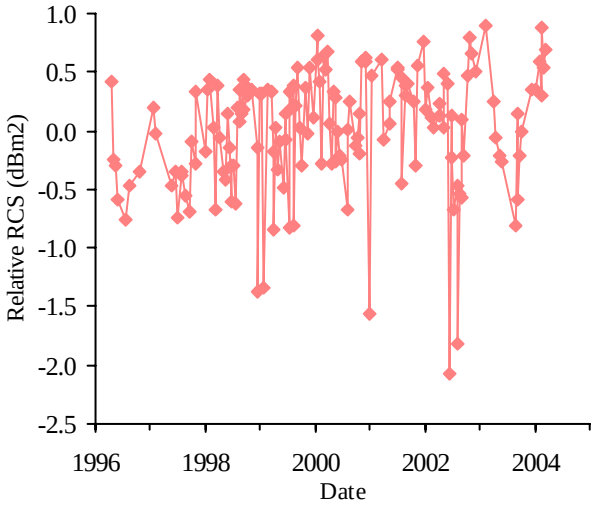

Fig. 6(c). Neustrelitz relative radar cross-section as a function of date

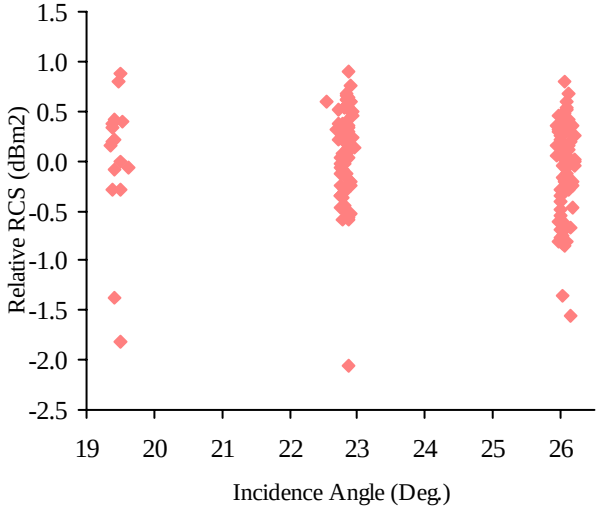

Fig. 6(d). Neustrelitz relative radar cross-section as a function of incidence angle

ADC Power Loss Correction

ERS-2 SAR raw data are quantised to 5 bits within the on-board Analogue to Digital Convertor (ADC). The distribution of the I and Q channels is Gaussian and so if the input signal is high, a large number of data values will occupy the lowest and highest quantisation levels, i.e. saturation will occur. Any saturation will lead to the situation where the output power from the ADC will be less than the input power (i.e. there is a power loss). The gain of the ERS-2 SAR is such that a proportion of imagery is affected by saturation (for I and Q raw data standard deviations greater than approximately 5.3) but this proportion is significantly less than that for ERS-1 SAR imagery due to the reduced gain of ERS-2 compared to ERS-1. An ADC power loss of more than 1dB occurs if the I and Q standard deviation is greater than approximately 9 and a saturation level of more than approximately 6%).

Noise Equivalent σ^o

The upper limit to the noise equivalent σ^o ($NE\sigma^o$) of an image can be estimated by measuring the radar cross-section of low intensity regions (usually ocean/inland water regions). Fig. 7(a) shows low intensity region radar cross-section measurements from ERS-2.SAR.PRI images (after removing the range dependence in $NE\sigma^0$ due to the elevation antenna pattern, range spreading loss and $\sin(\alpha)/\sin(23°)$ to give a $NE\sigma^0$ at the mid-swath position). The noise measurements after the gain changes at the end of February 2003 are coloured red.

The trend line is for a 0.66dB per year decrease in transmitter pulse power between launch and the end of 2000, a decrease of 0.82dB per year until the end of February 2003, a 3dB drop at the end of February 2003 and then the resumption of the 0.66dB per year decrease. An offset of 26.3dB has also been used for the trend line; -26.3dB represents the noise equivalent radar cross-section at the start of the ERS-2 mission. Note that during mid-2000 and since mid-2001 there are $NE\sigma^0$ values below the trend line - this is due to imagery being used with higher replica and calibration pulse powers than the general downward trend in these powers. The $NE\sigma^0$ measurements indicate an estimated ERS-2 $NE\sigma^o$ of -26.3dB in July 1995, -21.0dB in early 2003 (i.e. an increase of just over 5dB in 7½ years) and -23.3dB in early 2004. This is similar to the change in transmitter pulse power over the same period (as measured by the calibration pulse power).

Assuming that the noise is thermal in origin, then the $NE\sigma^o$ is expected to change across the swath for PRI products due to the application of the elevation antenna pattern. It has been possible to select an ERS-2.SAR.PRI product with a low backscatter region extending from near to far range. Fig. 7(b) shows the low intensity region σ^o measurements for a 6km azimuth strip stretching from near to far range together with the ERS-2 SAR elevation antenna pattern with an offset of -23.5dB (and again after including the range spreading loss and incidence angle correction). It can be seen that the elevation pattern and the σ^o profile fit very well indicating that the noise is indeed thermal in origin.

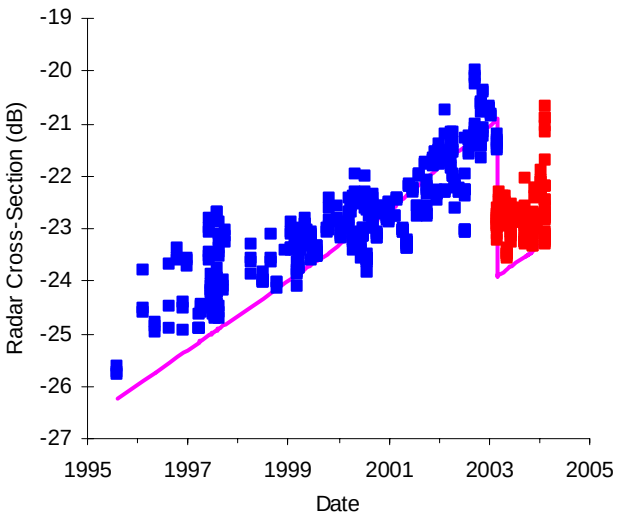

Fig. 7(a). ERS-2.SAR.PRI Noise Equivalent σ^o

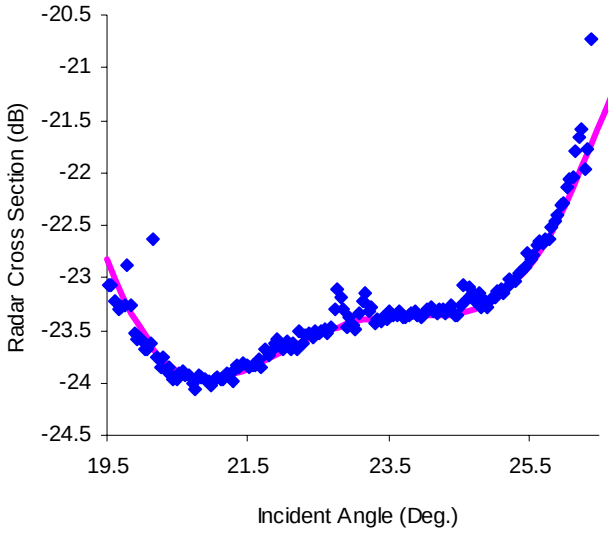

Fig. 7(b). ERS-2.SAR.PRI Noise Equivalent σ^o from Orbit 16652, Frame 2403

Nominal Replica Pulse Products

A small number of PAF SAR Verification Mode Processor (VMP) products (< 1%) are generated using a nominal replica pulse rather than a replica generated at the time of imaging (an extracted replica). Products generated with a nominal replica have significantly higher pixel values than products generated using an extracted replica. These products can be corrected. For ERS-2 SAR products, the correction depends on the extracted replica pulse power at the time of data acquisition. This can be estimated from the quarterly averaged values given in Table VI (based on replica pulse powers at the start of imaging sequences as shown in Fig. 3(b) - values based on ERS-2 high rate products can be found in [9]). For 2003 Q1, two corrections are given, one before 26th February and the other after 28th February due to the gain change between these dates. The correction factor is applied such that the image intensity values need to be reduced. More details can be found in [2, 5].

Year	Q1	Q2	Q3	Q4
1995			23.57	23.38
1996	23.23	23.15	23.05	22.78
1997	22.61	22.43	22.29	22.11
1998	21.97	21.81	21.57	21.42
1999	21.29	21.15	20.98	20.78
2000	20.60	20.47	20.44	20.21
2001	20.02	19.90	19.67	19.40
2002	19.19	19.21	18.90	18.63
2003	18.44, 21.52	21.49	21.33	21.10
2004	20.91			

Table VI. Quarterly averaged nominal replica pulse correction for the ERS-2 SAR (dB)

DISTRIBUTED TARGET RADAR CROSS-SECTION DERIVATION

The expression required to calculate the radar cross-section of a distributed target from ERS-2.SAR.PRI imagery is:-

$$\sigma^o = \frac{< A^2 >}{K_{PRI}} \frac{\mathrm{Sin}\alpha_D}{\mathrm{Sin}\alpha_{Ref}} \mathrm{PowerLoss} \quad (1)$$

where:-

σ^o = distributed target radar cross-section,

$<A^2>$ = average pixel intensity of a distributed target,

A = pixel digital number,

K_{PRI} = PRI calibration constant,

α_D = distributed target incidence angle (including any local surface slope),

α_{Ref} = reference incidence angle (23°),

Power Loss = ADC power loss.

The expression required to calculate the radar cross-section of a distributed target from detected complex data is different from the PRI products. This is because no elevation antenna pattern correction or range spreading loss has been applied to the SLCI products. For detected ERS-2.SAR.SLCI products the required expression is:-

$$\sigma^o = \frac{< A^2 >}{K_{SLCI}} \frac{\mathrm{Sin}\alpha_D}{\mathrm{Sin}\alpha_{Ref}} \mathrm{PowerLoss} \frac{1}{G(\theta_D)^2} \frac{R_D^3}{R_{Ref}^3} \quad (2)$$

where in addition to the terms used for PRI distributed target radar cross-section derivation:-

K_{SLCI} = SLCI calibration constant,

$G(\theta_D)^2$= elevation antenna pattern gain at the distributed target,

θ_D = distributed target look angle,

R_D = distributed target slant range,

R_{Ref} = reference slant range (847.0 km).

The method for calculating the ADC power loss is slightly different from the PRI product as it considers the fact that detected SLCI imagery is in slant range and has no elevation antenna pattern or range spreading loss applied.

Specific details of how to calculate the radar cross-section of distributed targets (including the ADC power loss) for ERS-2 SAR PRI and SLCI products can be found in [5].

POINT TARGET RADAR CROSS-SECTION DERIVATION

The expression required to calculate the radar cross-section of a point target from ERS-2.SAR.PRI imagery is:-

$$\sigma = \frac{I_P}{C_F}\frac{P_A}{K_{PRI}}\frac{\mathrm{Sin}\alpha_P}{\mathrm{Sin}\alpha_{Ref}}\mathrm{PowerLoss} \tag{3}$$

where in addition to the terms used for distributed targets:-

σ = point target radar cross-section,

I_P = total power in the point target mainlobe,

C_F = relative power in the point target sidelobes = 1/(1+ISLR),

ISLR = integrated sidelobe ratio,

P_A = PRI product pixel area (156.25m^2),

α_P = point target incidence angle.

Point target radar cross-section derivation from ERS-2.SAR.SLCI products requires that the data is resampled to preserve all the statistical properties of the data. This is needed to ensure that the detected image is adequately sampled (i.e. at twice per resolution cell). As the ERS SAR complex data is sampled at once per resolution cell, a resampling factor of two is required. It is also necessary to ensure that the complex data power spectra is completely within the sampling window. If the power spectra is 'folded over' from one end of the sampling window to the other, then a spectrum shift is required. In the case where only the mean intensity of a distributed target is required (such as for the distributed target radar cross-section calculation) then it is possible to detect the complex data without resampling.

For detected ERS-2.SAR.SLCI products the required expression is:-

$$\sigma = \frac{I_P}{C_F}\frac{P_A}{K_{SLCI}}\frac{1}{\mathrm{Sin}\alpha_{Ref}}\frac{1}{S_F^2}\mathrm{PowerLoss}\frac{1}{G(\theta_P)^2}\frac{R_P^3}{R_{Ref}^3} \tag{4}$$

where in addition to the terms used for PRI point target radar cross-section derivation:-

P_A = SLCI product pixel area (~30.8m^2),

K_{SLCI} = SLCI calibration constant,

S_F = sampling factor for detection of SLCI data,

$G(\theta_P)^2$ = elevation antenna pattern gain at the point target,

θ_P = point target look angle,

R_P = point target slant range.

The derivation of the ADC power loss corrections are the same as for distributed targets.

ATTITUDE AND DOPPLER VARIATIONS

ERS-2 was piloted in the nominal yaw steering mode using 3 gyroscopes out of a total of 6 available on board since launch until February 2000. During this period, there were several problems and failures with some of the 6 gyroscopes available on board of ERS-2. On-board software was developed to enable ERS-2 to be piloted in yaw-steering mode with a single gyro and thus to ensure continuity of operations in the case of additional gyroscope problems or failures. During the period from February 2000 to mid January 2001, the piloting of the ERS-2 satellite was performed using just one gyroscope (1GP) instead of the usual three gyroscopes. A consequence of this change was a loss of attitude stability but the impact of this on SAR product quality was small and no degradation in radiometric stability, as measured using the ESA transponders, was found [7]. During this period, the Doppler Centroid frequency increased for localised areas and time intervals but values were mostly limited to the first ambiguity number (-1600Hz to 1600Hz).

During this period, a new on board software to pilot the satellite without using any gyroscope but exploiting the capabilities of the Digital Earth Sensor and Digital Sun Sensor, was developed and tested. A first coarse version of this

software, the Extra Backup mode (EBM), was uploaded in December 2000 as a first step for gyro-less operations, and operationally used since mid January 2001 due to further problems with the remaining gyroscopes. Significant degradation of ERS-2 attitude occurred during the EBM. Fig. 8 shows the yaw, pitch and Doppler Centroid frequency since the start of 2000 and shows the large yaw and Doppler Centroid frequencies during the EBM. Very large Doppler Centroid frequencies are difficult to estimate in SAR processors - this is particularly the case for values outside the interval ±4500Hz with the ESA VMP processor. However, if the Doppler ambiguity number is properly estimated, even if it is high, then there is no impact on product quality - otherwise the image is de-focussed and miss-located in azimuth [8]. Only products with Doppler Centroid frequencies within ±4500Hz have been directly distributed to users. Products with Doppler frequencies outside this range were sent to the Product Control Service (PCS) at ESRIN for correct Doppler verification before delivery to users. Verification of correct Doppler ambiguity estimation has now been included in the automatic quality control check performed at the PACs systematically on all products before delivery to the users.

Improvements in attitude control took place in June 2001 with the introduction of the Zero Gyro Mode (ZGM) and again in March 2002 with the ZGM-Yaw Control Monitoring (ZGM-YCM). Now more than 90% of the Doppler Centroid frequencies remain within ±4500Hz (see Fig. 8(c)). Since the implementation of ZGM-YCM, the yaw values derived in near-real time from wave mode data are used to automatically correct the instrument attitude during the next orbit pass if necessary. Some changes to this strategy were required after the failure of the on-board tape recorder in June 2003, since data acquisition all over the orbit could not be ensured anymore. Using a network of receiving ground stations, it was possible to continue the low rate mission although coverage has been reduced to the north hemisphere. The new strategy used for routine yaw control monitoring is a so-called “regional yaw control monitoring” (R-YCM) as it is based on a limited set of data.

As it can be observed in Fig. 8, the changes in the low rate mission, and therefore on the data available for routinely monitoring the attitude, has not significantly impacted the Doppler evolution in time.

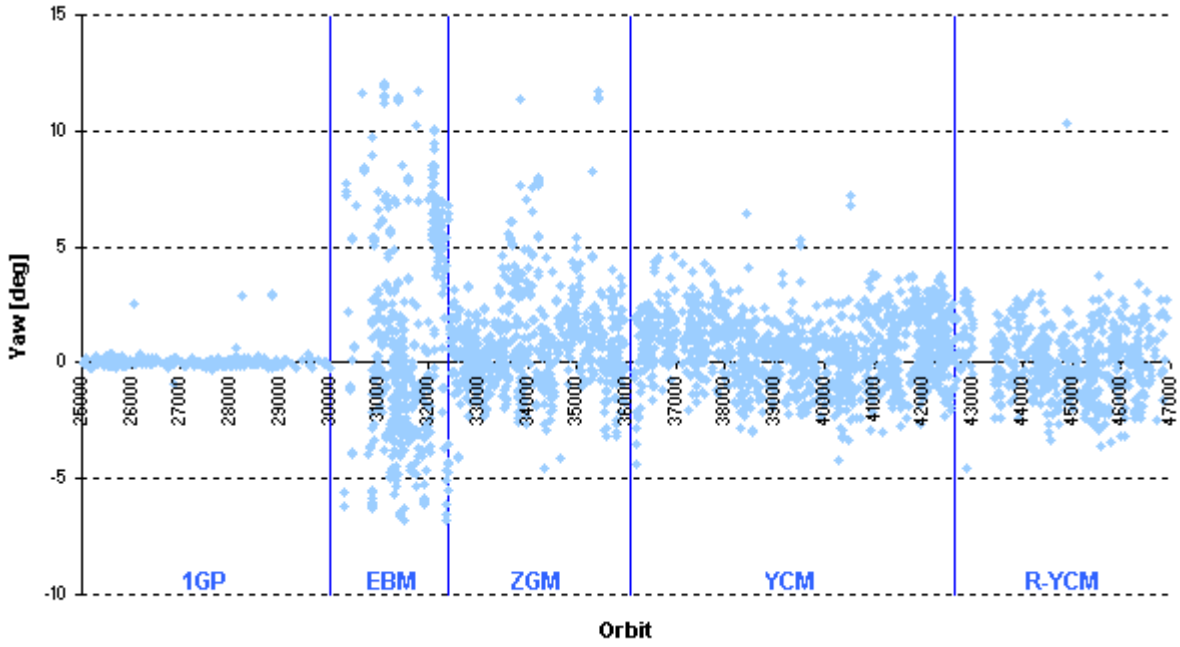

Fig. 8(a). ERS-2 Yaw Evolution (degrees) since January 2000.

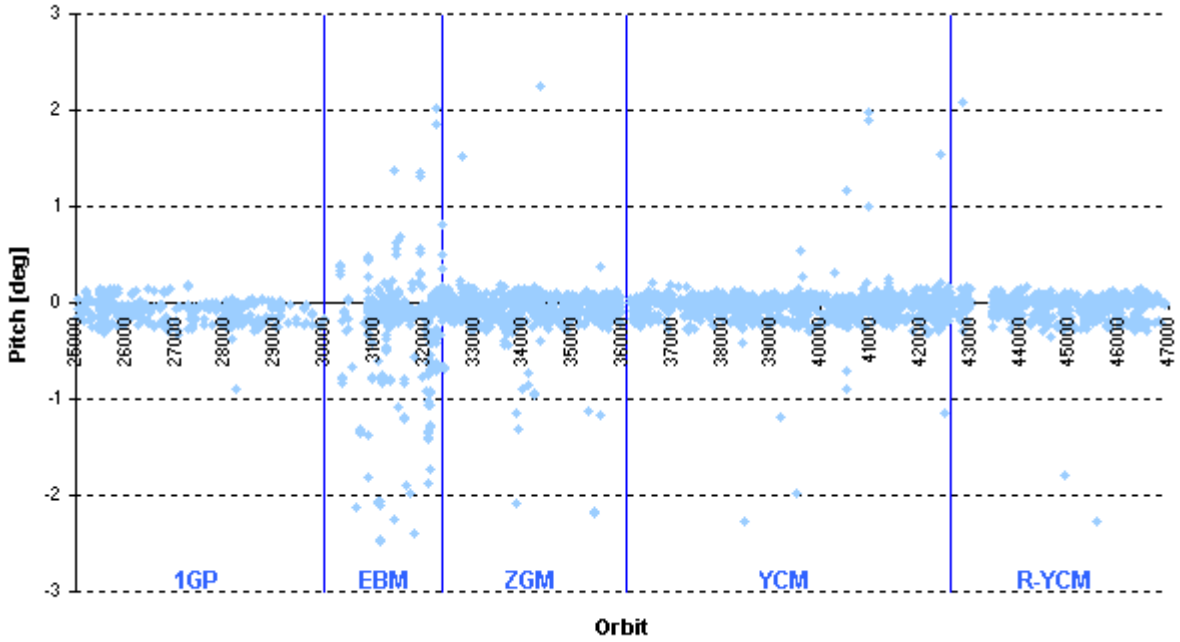

Fig. 8(b). ERS-2 Pitch Evolution (degrees) since January 2000.

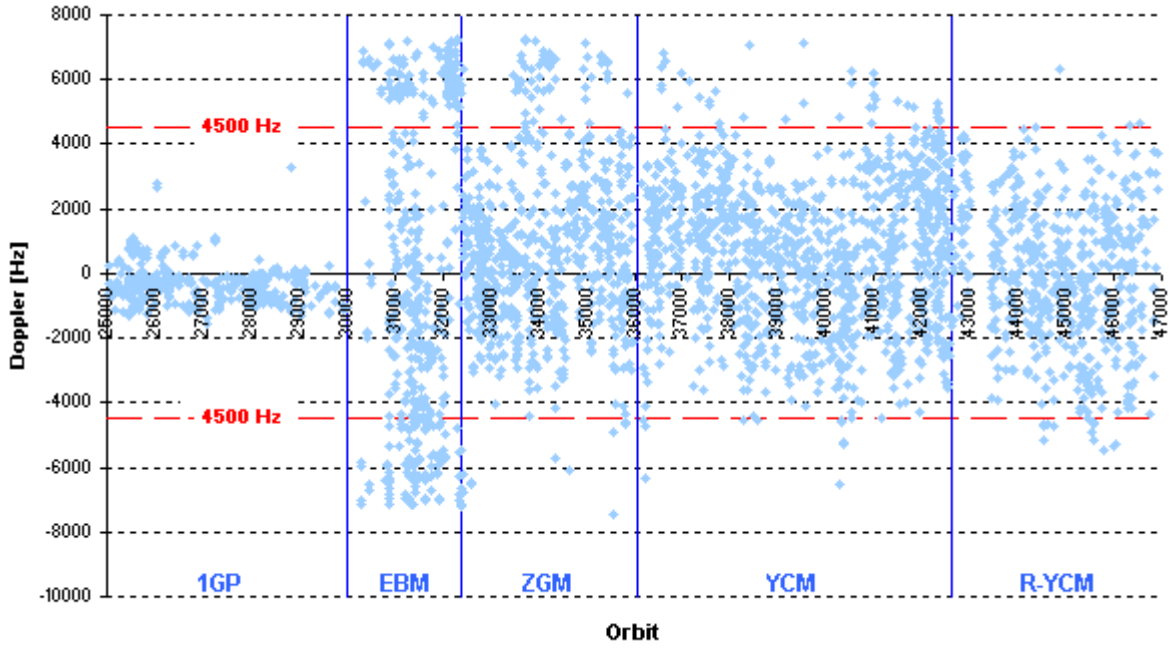

Fig. 8(c). ERS-2 Doppler Centroid Evolution (Hz) since January 2000.

With the start of single gyroscope operations in February 2000, a new criteria appeared for the selection of ERS-2 InSAR data based on the Doppler Centroid frequency difference between the InSAR pair. Due to the large and rapid variations of Doppler frequency during the EBM period, InSAR applications are not recommended with EBM data. The Doppler evolution around the orbit has been derived for 1GP, ZGM and ZGM-YCM orbits (repeat cycle to repeat cycle) to assist users in the identification of ERS-2 data still suitable for InSAR. Doppler frequency values are included in the ESA EOLI and DESCW data catalogues and an interactive Doppler frequency query tool is available at http://earth.esa.int/pcs/

ers/sar/doppler/. As an example of the Doppler frequency changes during the ZGM-YCM, Fig. 9 shows the Doppler frequency for ascending and descending passes during repeat cycle 80 in December 2002 and January 2003.

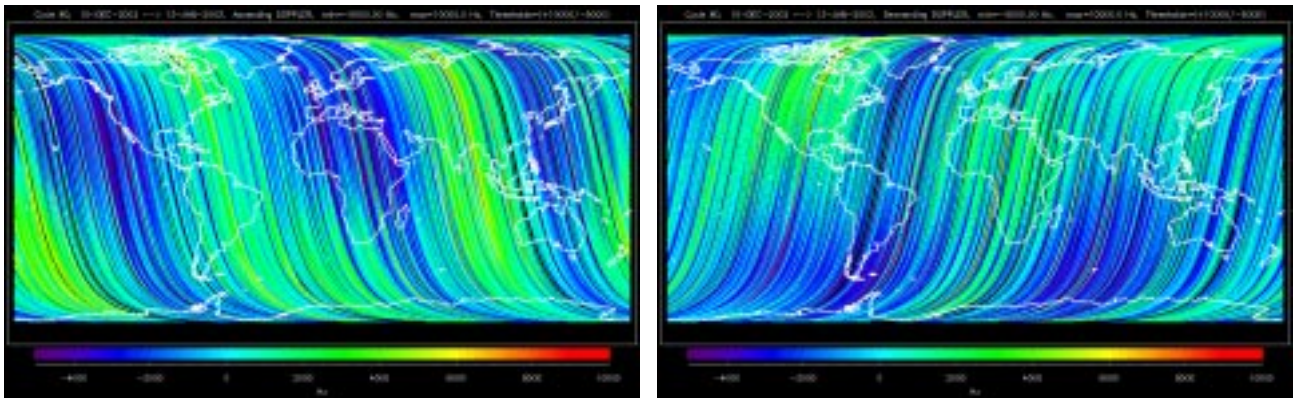

Fig. 9. ERS-2 Doppler Centroid Frequency during Repeat Cycle 80 (December 2002-January 2003) for ascending passes (left) and descending passes (right). Blue is -5000Hz and red is 10000Hz.

IMAGE LOCALISATION

Localisation of ERS-2 SAR imagery can be assessed by using the measured pixel coordinates of known point targets. This is achieved by converting the point target pixel coordinate to cartographic coordinates (x, y in a UTM map projection) via the image corner latitude and longitudes. The distribution of point target cartographic coordinates gives the image localisation (after compensation of terrain height has been included). More details on the derivation of the image localisation can be found in [6].

The ESA transponders deployed in The Netherlands have been used to assess the ERS-2 SAR image localisation. Fig. 10 shows the displacement of each transponder in cartographic coordinates after compensating for terrain height and for the transponder time delay up to the end of 1999 (i.e. before the start of single and zero gyroscope operations). The mean displacement, i.e. the image localisation, from all measurements is 25.5m.

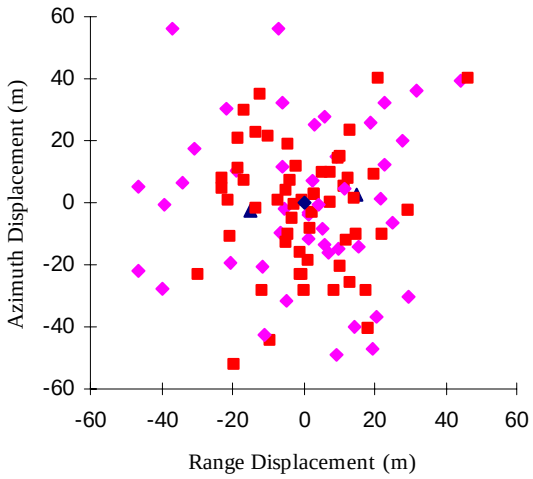

Fig. 10. ERS-2.SAR.PRI image localisation using the ESA transponders (blue triangles for transponder#1, purple diamonds for transponder#2 and red squares for transponder#3).

A detailed examination of ERS localisation can be found in [10].

CONCLUSIONS

This paper has given details of the performance of the ERS-2 SAR by consideration of quality assessment and radiometric calibration using the ESA transponder and two ERS ground receiving stations together with other aspect of the ERS-2 SAR and its products. Results presented show that the SAR worked well with excellent quality assessment and radiometric calibration results, although some products acquired during the Extra Backup Mode (the first half of 2001) have poor image quality due to degraded satellite attitude performance (these products have not been distributed to users). It has been shown that a consequence of the decrease in SAR transmitter pulse power at the rate of 0.66dB per year between launch and the end of 2000 and then 0.82dB per year until February 2003 has been a corresponding increase in the noise equivalent radar cross-section. Following the changes in the ERS-2 SAR gain at the end of February 2003, the NEσ^o was estimated to be -23.3dB in early 2004. Image localisation using the ESA transponders has been measured to be an excellent 25.5m.

ACKNOWLEDGEMENTS

Much of the ERS-2 SAR data used in this paper was processed at one of the ESA ERS Processing and Archiving Facilities. We would like to thank the staff at the UK-PAF for their support in the processing of this SAR data.

REFERENCES

[1] Meadows, P.J., Laur, H., Rosich, B. & Schättler, B., "The ERS-1 SAR Performance: a Final Update", Proceedings of the CEOS SAR Workshop, Tokyo, Japan, on 2-5 April 2001. *NASDA publication EORC-061*.

[2] Meadows, P.J., Laur, H., Sánchez, J.I. & Schättler, B., "The ERS SAR Performances", Proceedings of the CEOS SAR Workshop, 3-6 February 1998, ESTEC, Noordwijk, The Netherlands, *ESA publication WPP-138*, pp 223-232.

[3] Meadows, P.J., Laur, H. & Schättler, B., "The Calibration of ERS SAR Imagery for Land Applications", Proceedings of the 2nd International Workshop on Retrieval of Bio- & Geo-physical Parameters from SAR Data for Land Applications, 21-23 October 1998, ESTEC, Noordwijk, The Netherlands, *ESA publication SP-441*, pp 35-42.

[4] Meadows P.J., Laur, H. & Schättler, B., "The Calibration of ERS SAR Imagery for Land Applications", *Earth Observation Quarterly*, No 62, June 1999.

[5] Laur, H., Bally, P., Meadows, P., Sánchez, J., Schättler, B., Lopinto, E. & Esteban, D., "ERS SAR Calibration: Derivation of σ^0 in ESA ERS SAR PRI Products", ESA/ESRIN, ES-TN-RS-PM-HL09, Issue 2, Rev. 5e, February 2003.

[6] Meadows, P.J., "The Use of Ground Receiving Stations for ERS SAR Quality Assessment", Proceedings of the CEOS SAR Workshop, 26-29 October 1999, Toulouse, France. *ESA publication SP-450*, pp 525-530.

[7] Rosich, B., Esteban, D., Emiliani, G., Meadows, P., Scháttler, B., "Assessment of the new ERS-2 mono-gyro piloting mode on the quality of ERS SAR data and ERS SAR applications performance", ERS-Envisat Symposium, Gothenburg, Sweden, 16 - 20 October 2000. *ESA publication SP-461*.

[8] Rosich, B., Meadows, P.J., Schättler, B., Grion. M. & Emiliani, G., "The ERS-2 mono-gyro and extra backup piloting modes: impact on SAR performance", Proceedings of the CEOS SAR Workshop, Tokyo, Japan, on 2-5 April 2001. *NASDA publication EORC-061*.

[9] ESA Product Control Service, "Replica pulse power correction factor", http://earth.esa.int/pcs/ers/sar/calibration/replica_pwr/

[10] Mohr, J.J & Madsen, S,N., "Geometric calibration of ERS Satellite SAR Images", *IEEE Trans. GeoSci. Remote Sensing*, vol 39, pp 842-850, April 2001.